

DOE/NASA/1040-80/12
NASA TM-81442

(NASA-TM-81442) OVERVIEW OF A STIRLING
ENGINE TEST PROJECT (NASA) 27 p
HC A03/MF A01

N80-18564

CSCL 10B

Unclass

G3/44 47382

OVERVIEW OF A STIRLING ENGINE TEST PROJECT

Jack G. Slaby
National Aeronautics and Space Administration
Lewis Research Center

Work performed for
U.S. DEPARTMENT OF ENERGY
Conservation and Solar Applications
Transportation Energy Conservation Division

Prepared for
Fifth International Automotive
Propulsion Systems Symposium
Dearborn, Michigan, April 14-18, 1980



NOTICE

This report was prepared to document work sponsored by the United States Government. Neither the United States nor its agent, the United States Department of Energy, nor any Federal employees, nor any of their contractors, subcontractors or their employees, makes any warranty, express or implied, or assumes any legal liability or responsibility for the accuracy, completeness, or usefulness of any information, apparatus, product or process disclosed, or represents that its use would not infringe privately owned rights.

DOE/NASA/1040-80/12
NASA TM-81442

OVERVIEW OF A
STIRLING ENGINE
TEST PROJECT

Jack G. Slaby
National Aeronautics and Space Administration
Lewis Research Center
Cleveland, Ohio 44135

Prepared for
U. S. DEPARTMENT OF ENERGY
Conservation and Solar Applications
Transportation Energy Conservation Division
Washington, D. C. 20545
Under Interagency Agreement EC-77-A-31-1040

Fifth International Automotive
Propulsion Systems Symposium
Dearborn, Michigan, April 14-18, 1980

OVERVIEW OF A STIRLING ENGINE TEST PROJECT

Jack G. Slaby

National Aeronautics and Space Administration
Lewis Research Center
Cleveland, Ohio

ABSTRACT

The NASA Lewis Research Center has overall project management responsibility for the Department of Energy Stirling Engine Highway Vehicle Systems Program. As part of this program the Lewis Research Center is conducting tests on three Stirling engines ranging in size from 1.33 to 53 horsepower (1 to 40 kW). The results of these tests are contributing to the development of a broad base of Stirling engine technology. In addition, the tests are directed toward developing alternative, backup component concepts to improve engine efficiency and performance or to reduce costs. Some of the activities include investigating attractive concepts and materials for cooler-regenerator units, installing a jet impingement device on a Stirling engine to determine its potential for improved engine performance, and presenting performance maps for initial characterization of Stirling engines. This report presents some of the experimental results to date and predictions of results of tests that will be conducted on these Stirling engines.

INTRODUCTION

The NASA Lewis Research Center has overall project management responsibility for the Department of Energy (DOE) Stirling Engine Highway Vehicle Systems Program. The major effort of this program is being performed by a team headed by Mechanical Technology, Inc., and including United Stirling of Sweden and AM General. In support of this engine development activity, the Lewis Research Center is conducting some in-house Stirling engine technology tests to develop alternative, backup component concepts for better engine efficiency and performance or lower costs. In addition, NASA funding is being used to develop a more general Stirling engine technology base at the Lewis Research Center through in-house and contractual efforts.

Currently, there are three Stirling engines under test at Lewis. The smallest - a 1.33-horsepower (1-kW) output free-piston, single-cylinder, Stirling engine - was purchased under NASA funding and just recently was brought on line for testing. Initial efforts will concentrate on characterizing the engine with a dashpot load.

A ground power unit Stirling engine (GPU-3), with a single-cylinder rhombic drive, was converted at Lewis to a 10-horsepower (7.5-kW) research configuration, under DOE funding. The engine was originally built by General Motors Research Laboratories for the U.S. Army in 1965 as part of a 4-horsepower (3-kW) engine-generator set. Reports have been published presenting GPU-3 data with an alternator as the load. The engine is currently connected to a dynamometer load because the alternator load limited the en-

gine power output. This engine is being used as a test bed for advanced Stirling engine component concepts. Regenerators and coolers of unique configurations and materials are being evaluated for improved performance and lower cost on this engine. In addition, a concept is being investigated whereby the heat-transfer coefficient can be increased on the combustion side of the heater tubes and thus provide an opportunity for lower combustion temperature with associated lower generation of nitrogen oxides.

A United Stirling 53-horsepower (40-kW), four-cylinder, double-acting engine, the P-40, is being tested as a part of the DOE project to establish baseline data for Stirling engine characterization. As part of this characterization, temperatures, pressures, and pressure-volume traces are recorded from the engine expansion and compressor spaces. Performance maps of engine power and efficiency are being generated, and steady-state emissions measurements are being obtained over a range of operating conditions. In addition, the Bureau of Mines, under an interagency agreement between NASA and the Department of the Interior, is funding some of the P-40 work in reduced emissions, durability assessment, and performance with helium as the working fluid.

This report presents some of the experimental results to date and predictions of results of tests that will be conducted on these Stirling engines.

FREE-PISTON STIRLING ENGINE

The RE-1000, designed and built by Sunpower, Inc., of Athens, Ohio, is an electrically heated, single-cylinder research engine with a dashpot load. The free-piston Stirling engine, an annular regenerator type of engine, was optimized with helium as the working fluid. The engine, pictured in figure 1 and shown schematically in figure 2, operates at 30 cycles per second (30 Hz) under 1015-ps_i (7.0-MPa) pressure. The purchase and test of this engine are being funded by NASA.

The 34 heater-head tubes were fabricated from 1/8-in. (0.32-cm) diameter Inconel 718I and were designed to operate at 1202° F (650° C). The heater head (fig. 1) is located (though somewhat hidden) below the flange in the center of the three vertical support members. The power piston mass is 13.4 pounds (6.1 kg), the displacer mass is 0.9 pound (0.41 kg), and the maximum stroke of each is about 1.6 inch (4 cm). The annular regenerator housing is filled with stainless steel fabricated by a knitting process. The regenerator porosity for this engine is 75.9 percent, and the metal wire diameter is 0.0035 inch (88.9 μm).

The gas side of the annular cooler is composed of 135 small, rectangular passages 0.02 by 0.150 inch (0.51 by 3.8 mm) wide by 3 3/8 inches (8.5 cm) long. The water side of the cooler, the same length, consists of 80 axial holes 0.120 inch (3 mm) in diameter staggered along two concentric bolt circles. The holes are drilled in an aluminum housing. Heat is transferred from the hot gas to the cooling water through about 1/4 inch (6.3 mm) of aluminum. Individual component location is schematically shown in

figure 2. In this design the displacer rod is stationary, and the diameter of the pressure vessel is 8 3/4 inches (22.2 cm). Both the displacer and the displacer rod are shown in figure 3; the power piston is shown in figure 4. Note the spider attached to the displacer rod. One end of the power piston is milled out to allow the power piston to extend into the spider during operation and thus eliminate some dead volume.

A schematic of the instrumentation layout is shown in figure 5. This arrangement permits a comprehensive determination of the engine characteristics. For example, the output power can be checked by measuring the power dissipated in the dashpot. This can be compared with the engine power measured by force and velocity transducers. The dashpot load is varied by adjusting an orifice contained in the dashpot.

A free-piston engine has the following advantages: The free-piston engine is a hermetically sealed unit that eliminates shaft sealing problems. A free-piston engine such as the RE-1000 could be modified to incorporate a linear alternator integral with the power piston to supply electric power. Reference 1 discusses such an arrangement. Also the RE-1000 could be modified to drive a hydraulic system, like the heart-pump free piston of reference 2. This modification requires the incorporation of a diaphragm element to separate the gas from the hydraulic fluid. The free-piston engine is inherently simple, with no need for a mechanical drive. The free piston engine thus has the potential for higher system efficiency because of the reduction in mechanical losses.

Another feature of the free-piston engine is the ability to accommodate load changes by self-adjusting the stroke. This simplifies the controls for a constant-frequency engine.

A typical performance map taken from the engine operating manual is shown in figure 6. Engine output power is plotted versus piston stroke. The working fluid is helium at 1015 psi (7.0 MPa), and the inlet coolant temperature is maintained at 80° F (27° C). This engine is a research engine designed for simplicity first and efficiency second. Nevertheless, efficiencies around 30 percent have been achieved. The RE-1000 engine is currently undergoing engine characterization. Future testing will consider replacing the dashpot load with either a hydraulic output device or a linear alternator.

COMPONENT EVALUATION USING THE GPU-3 STIRLING ENGINE

The NASA Lewis Research Center has presented low-power (<6 hp, 4.5 kW) test results from the GPU-3 Stirling engine in references 3 to 5. This engine was originally built by General Motors Research Laboratories for the Army in 1965 as part of a 4-horsepower (3-kW) engine-generator set designated GPU-3. Recently a dynamometer has replaced the current-limited alternator as the engine load in order to absorb the full power output of the engine. The engine and dynamometer are shown in figure 7. The GPU-3 engine is a single-cylinder displacer engine with a rhombic drive and sliding rod-seals. It is capable of producing a maximum of approximately 10 horsepower

(7.5 kW) with hydrogen working fluid at 1000-psi (6.89-MPa) mean working space pressure.

Component evaluation tests are being conducted on this engine with a highly instrumented heater head. These measurements, with advanced instrumentation, will serve as a baseline for component testing, which will require comparisons of temperature and pressure measurements at the interfaces of these components. Comparing measured parameters is necessary because comparing components on the basis of engine efficiency and engine output power may not be reliable for certain components. The reason is that these components are being evaluated in a fixed-design engine, which may mask their possible gains. Thus a component may have potential benefits that would not show a performance gain on the GPU-3 engine but would in a reoptimized engine.

Several components have been selected for evaluation in the GPU-3 engine. These tests are being conducted as part of the DOE-funded Small Engine Experiments in-house project at Lewis. The first component is the Schladitz regenerator.

Schladitz Regenerators

Schladitz regenerators use a matrix made up of Schladitz-Whiskers. This high-strength filamentary material was developed in Germany by Professor Herman J. Schladitz. The regenerators being evaluated in the GPU-3 engine were fabricated by the Research Laboratories for the Engineering Sciences School of Engineering and Applied Science, University of Virginia. The whisker, which is not monocrystalline, is characterized by extremely small crystallite size and a large number of defects in the crystal lattice of its structure. Schladitz-Whiskers are produced by chemical vapor deposition. This process is well established and widely practiced. The end product is a polycrystalline metal whisker with a diameter that is controllable between less than 3.9 microinches (0.1 μm) and greater than 0.0059 inch (150 μm). The length-diameter ratio is also controllable to 10 000. The whisker size in individual batches is generally uniform. The other variable physical characteristics of the Schladitz-Whisker are surface-volume ratio, porosity of whisker matrix (a few percent to 95 percent), alignment of individual whiskers, smoothness of the whisker surface, and shape of whisker bodies.

For a typical heat exchanger, such as a Stirling engine regenerator, made from polycrystalline iron whiskers the wire diameter would range from 19.5 microinches to 0.00079 inch (0.5 to 20 μm). Figure 8 is a typical photomicrograph of a Schladitz-Whisker specimen. These whiskers can be sintered into bodies with porosities exceeding 95 percent and a large surface area. The composite has a high intrinsic strength. This strength prevents compression from the pressure of the fluid flowing through the matrix.

Schladitz-Whiskers are quite inexpensive in comparison to most other whiskers or filaments, as well as less costly than screens currently used for Stirling engine regenerators. The most recent estimates for commercial production of iron Schladitz-Whiskers are \$1 to \$10 per pound (\$2.2 to \$22

per kg) (ref. 6). The production of Schladitz-Whiskers is economical for two reasons: First, technical-grade gases can be used; and second, the yield from the process is high. The production is rapid since many small crystals take much less time to produce than a few large perfect crystals.

For comparison, figure 9 shows one of the eight cooler-regenerator units taken from the GPU-3 engine. In one regenerator there are 308 stacked screens of 200 mesh. Each screen is about 0.890 inch (2.26 cm) in diameter. The regenerator is 0.890 inch (2.26 cm) long. The total screen area in one regenerator is 1.33 square feet (0.124 m²). The cost for 200-mesh screen in January 1978 was \$2.43 per square foot (\$26.15/m²), or \$3.23 per regenerator (assuming no waste). On a per-pound basis the cost was about \$68 per pound (\$149.67 /kg) since there is about 0.047 pound (0.021 kg) of screen per regenerator. Thus on a per-pound basis the Schladitz-Whisker material at \$1 to \$10 per pound (\$2.2 to \$22 per kg) is considerably cheaper.

The performance of Schladitz regenerators is not expected to be significantly better than that of stacked-screen regenerators; the main advantage is cost reduction. Simplified calculations predict that the optimum Schladitz regenerator porosity is about 90 percent; and that whether stacked-screen or Schladitz regenerators are used, the indicated power and engine efficiency are about the same.

Figure 10 shows the indicated power and efficiency predicted for the GPU-3 engine as a function of regenerator porosity. The engine operating conditions are listed on the figure.

Figure 11 shows one of the Schladitz regenerator units fabricated for testing. Testing is expected to be started later in the year.

Duocell and Foil Fin Regenerator-Coolers

The Lewis Research Center, also under DOE funding, has awarded a contract to Energy Research and Generation (ERG) of Oakland, California, to design and fabricate advanced cooler-regenerators for testing in the GPU-3 Stirling engine. Two types of regenerator materials are being investigated, Duocell and Foil Fin. Only one will be chosen and tested on the GPU-3 engine.

Duocell. - An aluminum Duocell configuration is shown in figure 12. This sample has a porosity of 94 percent with 10 pores per inch (4 pores/cm). Different metal and much finer pore size would be used for the Stirling engine application. Duocell is fabricated from a melted base metal by using inert gas and a hard vacuum to directionally solidify the base metal into the Duocell matrix. The isotropic structure provides a heat-exchanger matrix with an extended surface area and a uniform-flow cross-sectional area.

A particular feature of Duocell is the flexibility to vary the basic structure. These variations include (1) the independent variation of vol-

ume fraction for constant cell size, (2) the variation of strand cross-section geometry, (3) the variation in degree of anisotropy in preferred directions, (4) the variation in cell size and/or density in preferred directions, and (5) the ability to produce Duocell with pore-free solid strands that are integral with solid surfaces that are either internal or external to the matrix at selected locations. Duocell can be made from most metals, ceramics, cermets, and plastics.

Foil Fin. - Foil Fin is a staggered off-set array of aerodynamically shaped airfoils that act as fins to provide a heat-exchanger matrix with an extended surface area. Figure 13 schematically shows a Foil Fin configuration. The Foil Fin is fabricated by a high-speed forming process in which both the cross section of the fins and the density of the matrix can be varied. Foil Fins are produced with pore-free solid fins that may be integral with solid surfaces for use in a plate-fin heat-exchanger array or may be produced as rows of interconnected bars that can be stacked to form a regenerator matrix. Foil Fins can be made from most metals in a manner that maximizes the heat transfer per unit of pressure drop. Foil Fins can be joined to other parts by conventional techniques such as sintering and brazing.

Discussions with ERG personnel suggest that the costs of Duocell and Foil Fins are about the same - that is, about four times the cost of the base metal under mass-production conditions.

Continuously Knitted Regenerator

Another interesting type of regenerator material is fabricated by the Metex Corp. of Edison, New Jersey. Figure 14 shows a representative sample of this material. The free-piston Stirling engine discussed in this report and fabricated by Sunpower of Athens, Ohio, contains this type of regenerator material. The matrix is formed from a single strand of continuously knitted stainless-steel wire. The knitting process is similar to that used in manufacturing nylon hosiery. A cylindrical body is produced that is then compressed into a square cross-sectional configuration as shown in the figure. This shape facilitates placing the material in an annular regenerator housing. The stainless-steel wire diameter ranges from 0.002 to 0.011 inch (0.005 to 0.028 cm). The porosity has been varied from 50 to 90 percent. Discussions with the company suggest that the regenerator material sells for about \$20 per pound (\$44/kg).

Jet Impingement

One of the advantages of a Stirling engine is low exhaust emissions. Even these low emissions could be reduced further if the combustion temperature were reduced. To reduce the combustion temperature while still putting at least the same amount of energy into the engine at the same heater tube temperature, the heat-transfer coefficient on the combustion side of the heater is increased. Stirling engines operating with either hydrogen or helium as the working fluid have a high heat-transfer coefficient on the inside wall of the heater tubes. The limiting resistance to heat transfer into the working fluid is the combustion-side heat-transfer coefficient.

Typically this value is on the order of one-tenth of that on the inside of the tubes.

Rasor Associates of Sunnyvale, California, has experience using jet impingement to enhance the heat-transfer coefficient on the combustion side of heat exchangers. This jet impingement technique is best described in the following manner.

The heater head of the GPU-3 Stirling engine is shown in figure 15. This engine has a single row of 80 circumferential heater tubes. The jet impingement concept is shown schematically in figure 16 as a silicon carbide jet shell inserted in the heater-tube array. The jet shell contains a large number of holes or jet nozzles (0.030 to 0.060 in. (0.76 to 1.52 mm) in diameter). The combustion gas inside the jet shell is forced through the jet nozzles and impinges on the heater-head tubes. The purpose of the directed jets is to break up the boundary layer on the surface of the tubes and thereby reduce the resistance to heat transfer. Previous jet impingement experience by Rasor Associates indicates that the heat-transfer coefficient can be increased by a factor of 2, though the pumping loss penalty may be excessive. Calculations were made using operating conditions from the GPU-3 engine with hydrogen as the working fluid. Combustion-gas temperatures are shown on the schematic diagram of figure 17 for a reference case (no jet impingement) and a projected jet impingement case. For the reference case the inlet-air and exhaust-gas temperatures were measured, as well as the heater-tube temperature. The other three temperatures shown around the loop were calculated. The combustion-side heat-transfer coefficient was calculated to be 60 Btu/hr ft² °F (340 W/m² °C). The same figure shows the calculated temperatures around the loop with jet impingement. For this case the same air-fuel ratio, fuel flow rate, heater-tube temperature, and inlet-air temperature as in the reference case were used; but the combustion-side heat-transfer coefficient increased by a factor of 2 to 120 Btu/hr ft² °F (680 W/m² °C). The combustion temperature was reduced significantly from 3439° F (1893° C) to 3053° F (1678° C). Under these conditions the amount of nitrogen oxides emissions should be reduced significantly. The calculations did assume variable combustion-gas specific heat but did not take into account any fouling of the outside of the heater tubes. Also radiation heat transfer from the silicon carbide shell to the heater tubes was neglected. The radiation should help in two ways (1) to increase the amount of heat transferred (approximately 10 percent) and (2) to heat the tubes more uniformly and thus minimize temperature variations.

Rasor Associates is fabricating a jet-impingement silicon carbide shell to be installed and tested on the GPU-3 engine. Figure 18 shows a predicted temperature performance map along with the power loss required to pump the gas through the jet shell. The estimated pumping power loss of 30 percent of the output power for an increase in the heat-transfer coefficient by a factor of 2 is prohibitive. Therefore a more realistic case is to increase the heat-transfer coefficient by 50 percent to 90 Btu/hr ft² °F (510 W/m² °C). Under these conditions the flame temperature is reduced to 3180° F (1749° C), a reduction sufficient to significantly reduce nitrogen oxides emissions, yet the 3 percent power loss is not prohibitive.

The heat-transfer-coefficient curve is drawn as a band rather than a line in figure 18 to take into account uncertainties such as flue gas properties and noncircular jet holes. In using the performance map the flame temperature and exhaust-gas temperature are determined by vertical lines from the appropriate heat-transfer coefficient. These vertical lines when extended to the abscissa also show the estimated pumping power required for jet impingement.

The degree of success of the device will be determined by measuring the inlet and exit temperatures on the preheater. The objective of this test is to demonstrate proof of concept.

In designing an engine with a jet impingement combustor, nitrogen oxides reduction need not be the only benefit. The heater-head heat-transfer surface area (number and size of heater tubes) could be reduced; this would lower the engine dead volume and improve engine performance. However, for the tests conducted at the Lewis Research Center a ground rule was established not to alter the heater head.

UNITED STIRLING P-40 ENGINE

A United Stirling four-cylinder, double-acting engine, the P-40, is being tested as part of the DOE project to establish baseline data for Stirling engine characterization. In addition the Bureau of Mines is funding some P-40 work in reduced emissions, durability assessment, and performance with helium as the working fluid.

A subsequent paper, currently being written, will discuss in detail the test results and engine operating experiences that have been accumulated during the operation of this engine. For the purpose of this overview, engine performance maps will be shown for the engine as received and tested and then compared to the engine performance after the regenerators became degraded from oil leakage past the rod-seals. In addition, regenerator calibration characteristics will be compared for regenerators as received and after oil contamination.

The P-40 engine and dynamometer in a Lewis test cell are shown in figure 19. The control room with supporting data acquisition and recording instrumentation is shown in figure 20. One of the heater-head quadrants with one cylinder and two regenerator housings is shown in figure 21. The involuted sections of the 18 heater tubes contain a spiral-wire fin; the straight section of heat-exchanger tubing contains conventional fins. Figure 22 shows the heater-head quadrant turned over, with the cylinder and regenerator housings exposed. The left cylinder housing contains the piston dome, and the piston and piston rings are shown in the foreground. The two regenerators (there are two regenerator-coolers per cylinder) are shown in their housings. The tubular cooler assemblies are located between the regenerators and the flow-plate housings.

One of the regenerators containing stacked stainless-steel screens is shown in figure 23, before it was used in the engine. A regenerator sub-

jected to oil resulting from leakage past rod-seals is shown in figure 24. The P-40 engine operated about 50 hours before the regenerators were removed because of oil-induced performance degradation. It is not known when the leakage occurred since it was apparently gradual. Attempts to clean an oil-contaminated regenerator in an ultrasonic solvent bath failed. The pressure drop actually increased. New rod-seals of an improved design have been installed in the engine, and this should greatly alleviate oil contamination.

Flow tests using air were conducted on the regenerators contaminated with oil as well as on clean as-received regenerators. All regenerators were subjected to airflow rates encompassing the dynamic head range encountered during hydrogen-charged engine operation. Figure 25 shows the performance degradation resulting from the oil-contaminated regenerators - one of which was shown in figure 24.

Matched sets of regenerators are used in the engine. Generally all eight regenerator, pressure drop - flow rate characteristic curves are identical. However, occasionally a regenerator deviated from the norm. The reason was fewer screens in the regenerator housing, as evidenced by a weight measurement comparison.

Figure 26 is a typical power-speed performance map for several engine operating pressure levels. These curves were taken from the P-40 acceptance test results. The performance penalty, as would be expected, is most severe at high speeds, where the pressure drop penalty becomes significant.

To better understand the engine behavior, some specialized instrumentation was added to the engine. One heater-head quadrant was instrumented to obtain expansion-space gas average temperature and dynamic pressure. Also transducers were added to measure average gas temperature and dynamic pressure in the compression spaces. With this improved capability we should be able to better understand the Stirling cycle behavior by analyzing dynamic pressure-volume maps from the expansion and compression spaces. In addition, on-line dynamic pressure and pressure drop data will be available for component analyses and computer code modeling.

CONCLUDING REMARKS

Stirling engine experimental test activities at the Lewis Research Center are predominantly a part of the Department of Energy automotive engine development project. The Bureau of Mines is funding some of the P-40 work in reduced emissions, durability assessment, and performance with helium as the working fluid. In addition, the free-piston engine testing described in this report is being funded directly by NASA as part of a more general Stirling engine technology activity. Currently three Stirling engines are under test at Lewis, ranging in size from 1.33 to 53 horsepower (1 to 40 kW).

The GPU-3 engine is being used as a test bed to evaluate several promising advanced components. Included in these activities are various unique regenerator concepts such as Schladitz-Whiskers, Duocell, or Foil Fin. A mesh regenerator knitted from a single continuous wire will be evaluated in

the free-piston engine. Jet impingement hardware is being installed for testing on the GPU-3 engine to determine its potential for engine efficiency improvement versus nitrogen oxides reduction.

The free-piston Stirling engine, though not nearly as advanced in technology as the kinematic engine, and with its own unique set of problems, nevertheless offers several potential advantages over the kinematic engine. These include a hermetically sealed unit (eliminating the rod-seal problem), mechanical simplicity, and the potential for high system efficiency. The RE-1000 engine is currently undergoing engine characterization testing.

The P-40 will eventually replace the GPU-3 engine as a test-bed engine at Lewis for in-engine performance evaluation of advanced components for automotive application. Currently the P-40 engine is being used to obtain baseline data for engine characterization, including performance maps and emission measurements. The P-40 tests are being conducted with engine-driven auxiliaries. Tests will be made to determine the power being consumed by these auxiliaries. Engine performance resulting from response to ramp or step changes will also be investigated, and the effects of different fuels and working fluids on engine performance will be assessed. The ratio of running-time to down time for the P-40 engine is expected to increase significantly with the installation of the improved rod-seals. Extensive on-line instrumentation and data acquisition and reduction equipment have been and are being installed to aid in evaluating and understanding engine operation and performance.

In summary, the three Stirling engines under test at the Lewis Research Center are contributing to our development of a broader base of Stirling engine technology. Although the testing is in the early stages, several attractive alternative component concepts are being evaluated, and computer predictions are being used to screen other potential component candidates. The early engine test results confirm our expectations that the Stirling engine is indeed a viable contender for automotive application.

REFERENCES

1. Dochat, George R.: Design Study of a 15 kW Free-Piston Stirling Engine - Linear Alternator for Dispersed Solar Electric Power Systems. (MIT 79TR47, Mechanical Technology, Inc.; DOE Contract DEN-3-56.) DOE/NASA/0056-79/1, NASA CR-159587, 1979.
2. Proposal to Continue Development of a Thermal Energy Converter for Implantable Circulatory Support Devices. Vol. 3, Annual Report Draft. JCGS/REL 7903-214, Univ. Washington, Mar. 1979.
3. Carrelli, J. E.; Thieme, L. G.; and Walter, R. J.: "Initial Test Results with a Single-Cylinder Rhombic-Drive Stirling Engine. DOE/NASA/1040-78-1, NASA TM-78919, 1978.
4. Thieme, Lanny G.; and Tew, Roy C., Jr.: "Baseline Performance of the GPU-3 Stirling Engine. DOE/NASA/1040-78-5, NASA TM-79038, 1978.
5. Thieme, Lanny G.: Low-Power Baseline Test Results for the GPU-3 Stirling Engine. DOE/NASA/1040-79-6, NASA TM-79103, 1979.
6. Neeley, Kay: An Overview of Schladitz-Whisker Technology. Univ. Virginia, Nov. 1979.

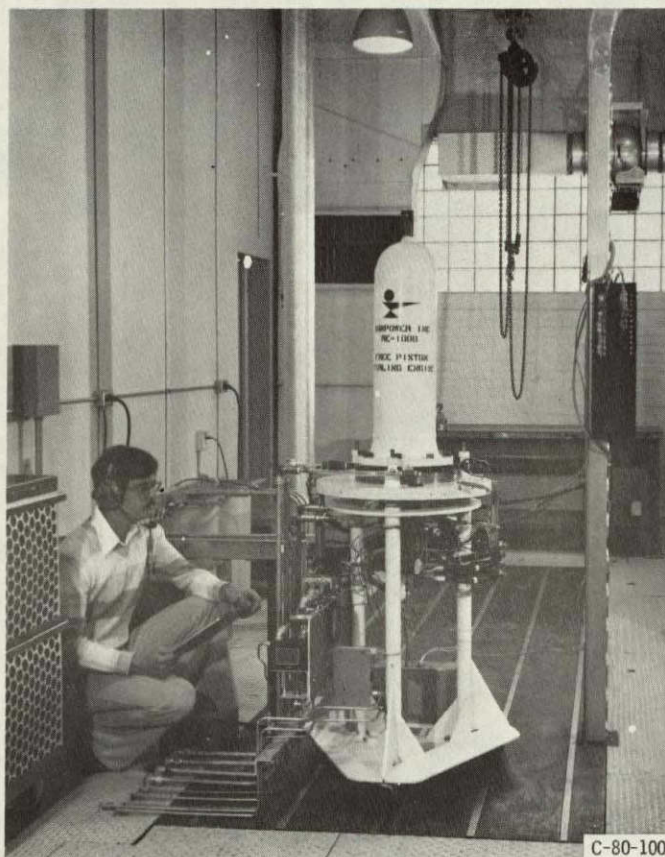


Figure 1. - RE-1000 free-piston Stirling engine.

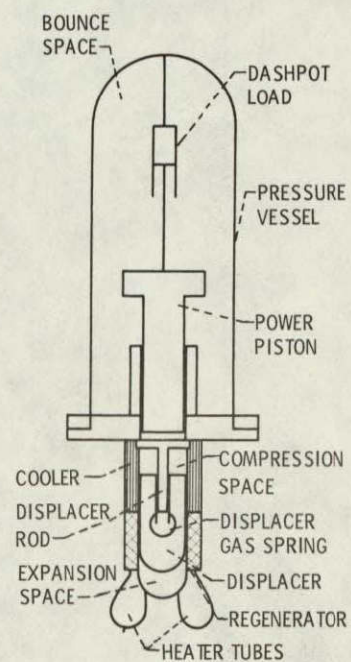


Figure 2. - Component layout of RE-1000 free-piston Stirling engine.

ORIGINAL PAGE IS
OF POOR QUALITY

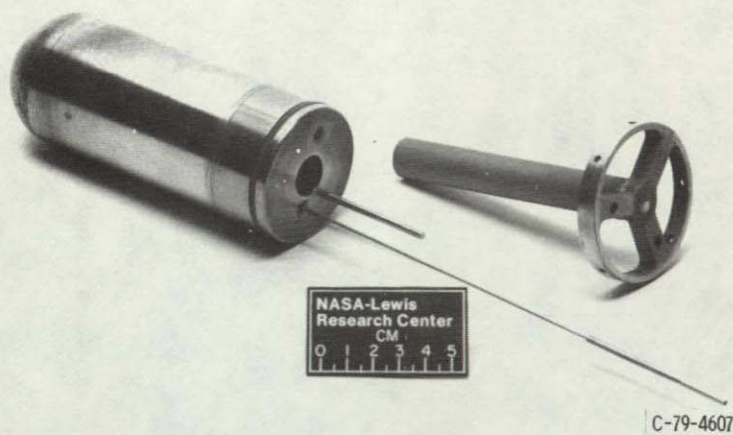


Figure 3. - Free-piston Stirling engine displacer and displacer rod.

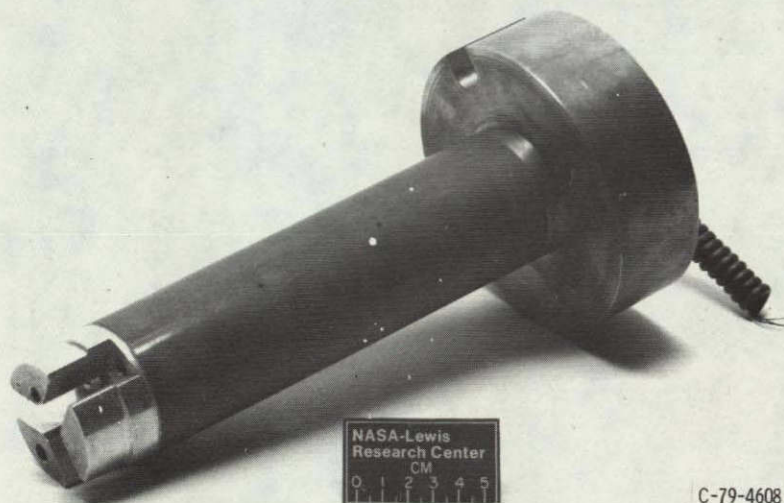


Figure 4. - Free-piston Stirling engine power piston.

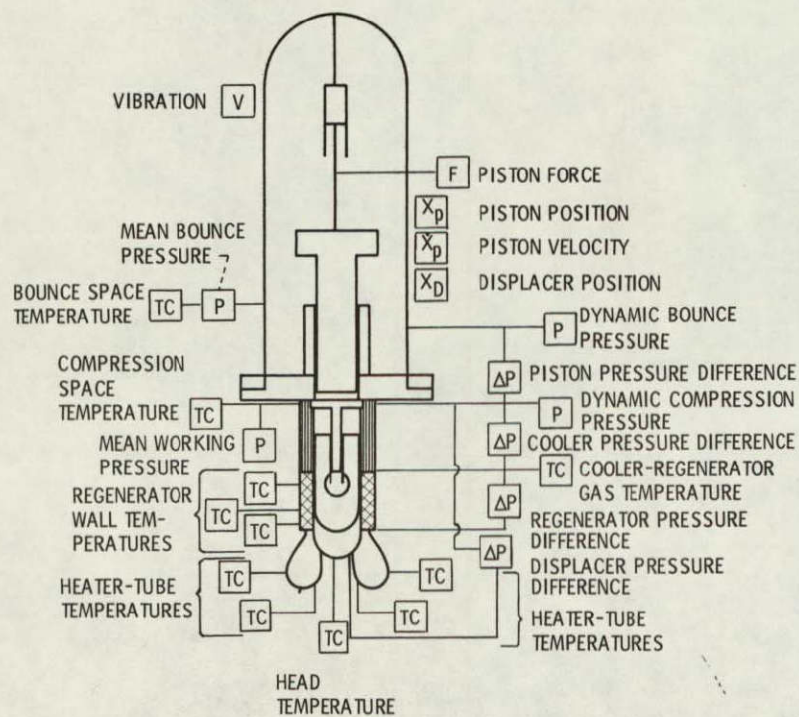


Figure 5. - Instrumentation layout of RE-100 free-piston Stirling engine.

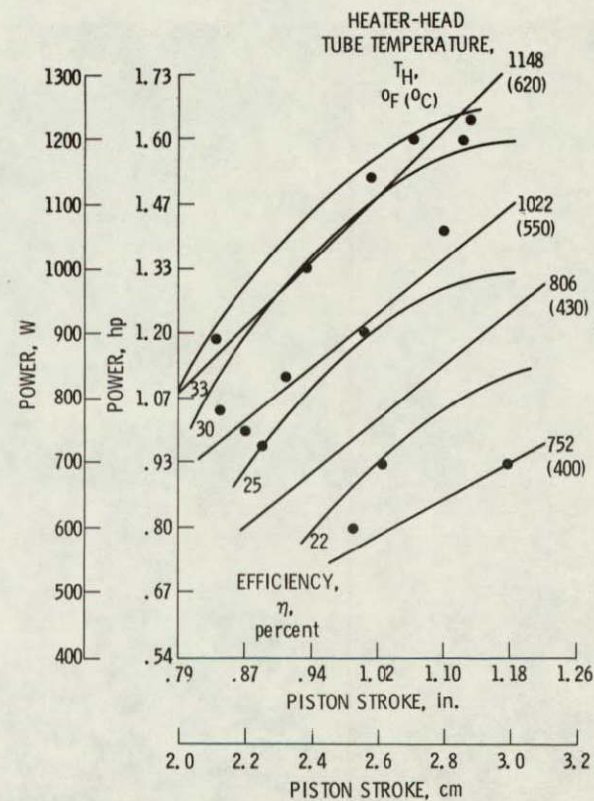


Figure 6. - Performance map of RE-1000 free-piston Stirling engine. Helium pressure, 1015 psi (7.0 MPa); coolant inlet temperature, 80° F (27° C); engine frequency, 30 cycles per second (30 Hz).

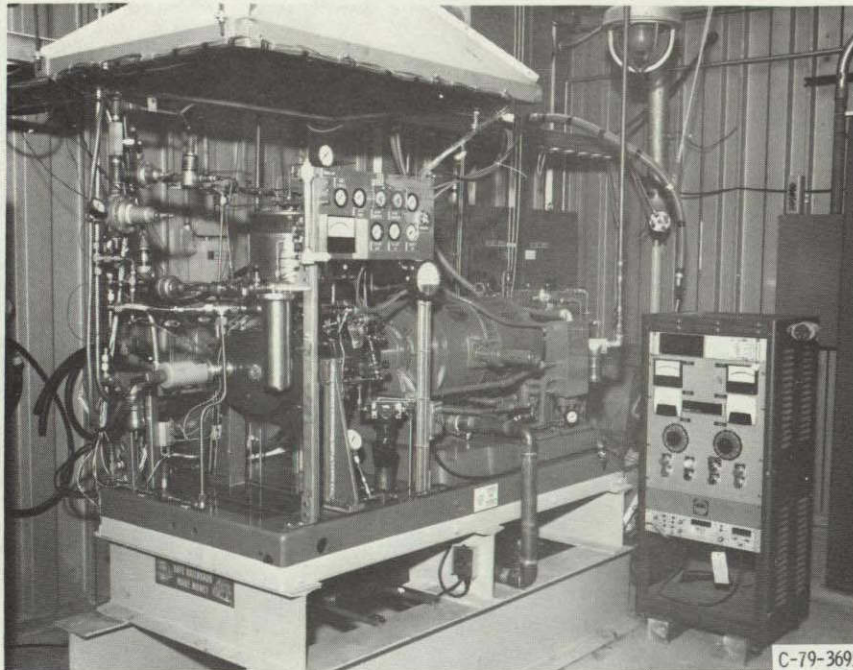


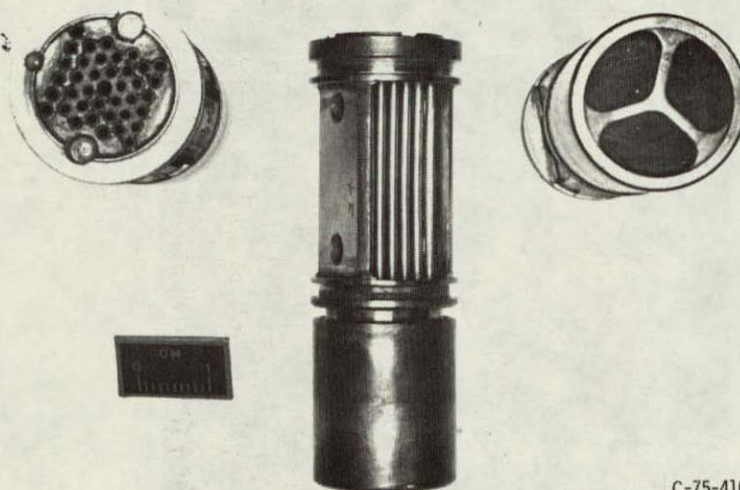
Figure 7. - GPU-3 engine connected to dynamometer load.



Figure 8. - Fine Schladitz-Whiskers in micrometer range used to produce whisker skeletons. Porosity, >95 percent.

ORIGINAL PAGE IS
OF POOR QUALITY

ORIGINAL PAGE IS
OF POOR QUALITY



C-75-4103

Figure 9. - GPU-3 cooler-regenerator cartridge assembly.

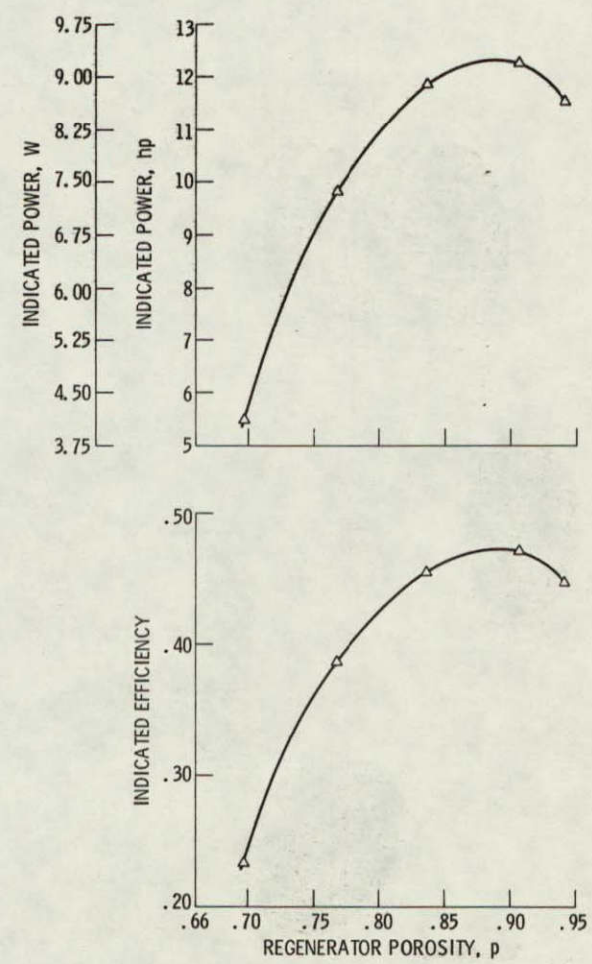
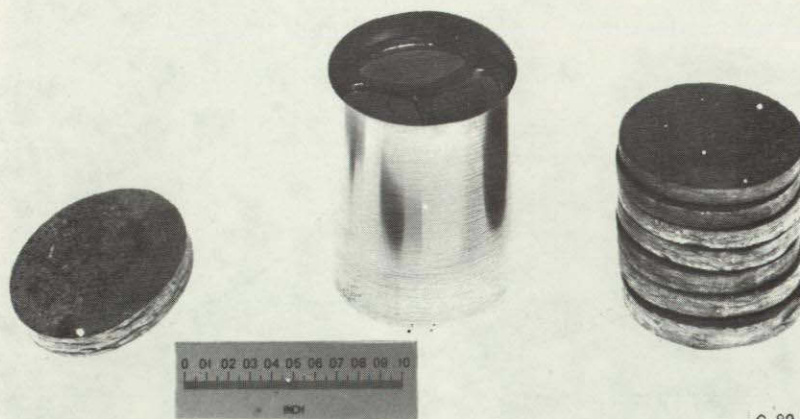
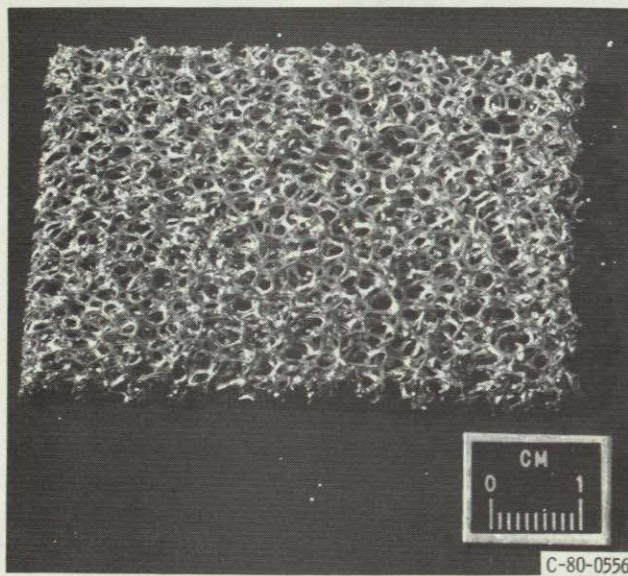


Figure 10. - Calculated efficiency and power of GPU-3 engine using Schladitz-Whisker regenerators. Working fluid, hydrogen at 1000 psi (6.89 MPa); heater-tube temperature, 1403° F (762° C); cooler-tube temperature, 165° F (74° C); engine speed, 3000 rpm (50 Hz); whisker diameter, 0.0004 in. (10 μ m).



C-80-0597

Figure 11. - Typical Schladitz-Whisker regenerator for GPU-3 engine.



C-80-0556

Figure 12. - Sample of aluminum Duocell material.

ORIGINAL PAGE IS
OF POOR QUALITY

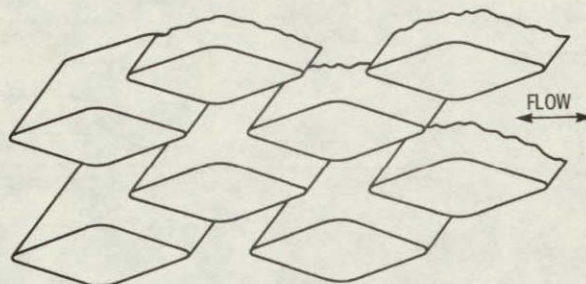


Figure 13. - Typical Foil Fin geometric configuration.

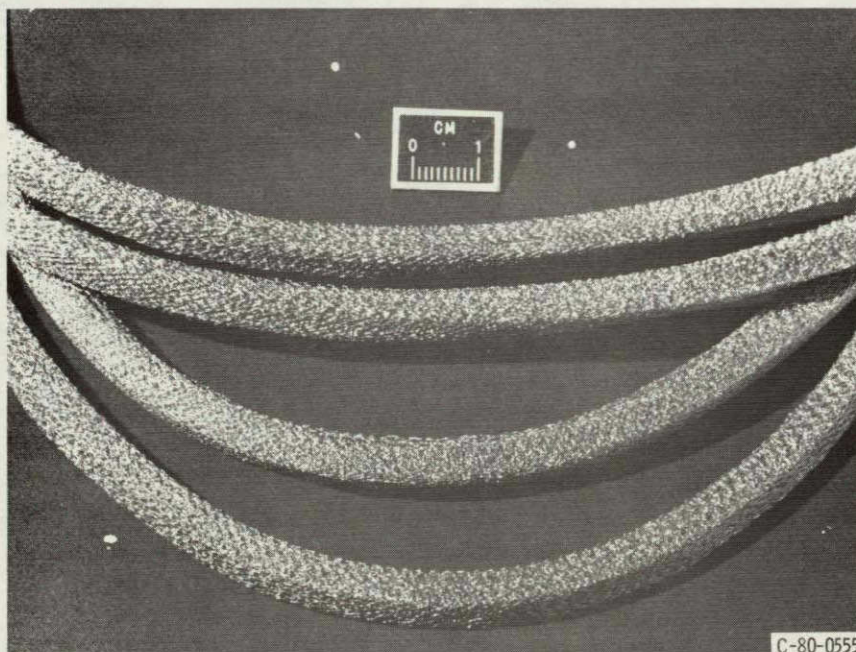


Figure 14. - Single strand of continuously knitted stainless-steel regenerator material.

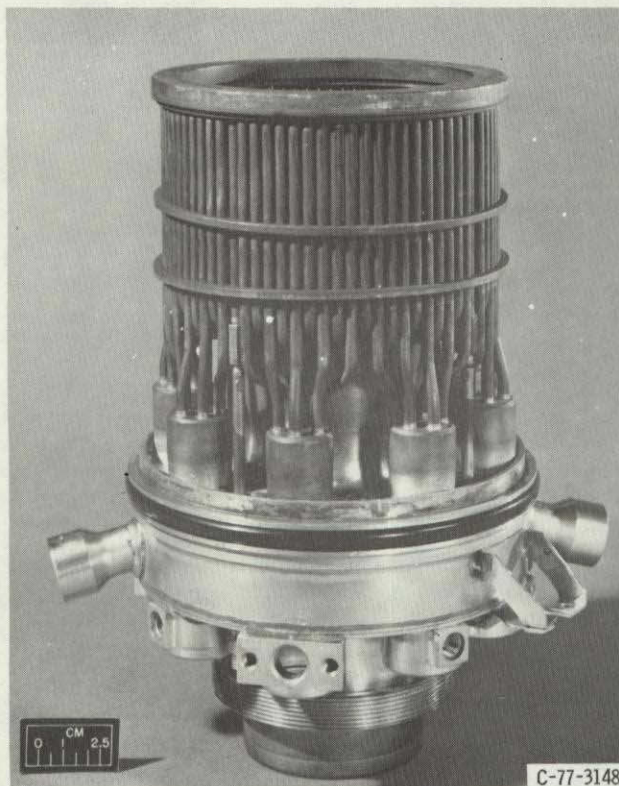


Figure 15. - GPU-3 heater-head assembly.

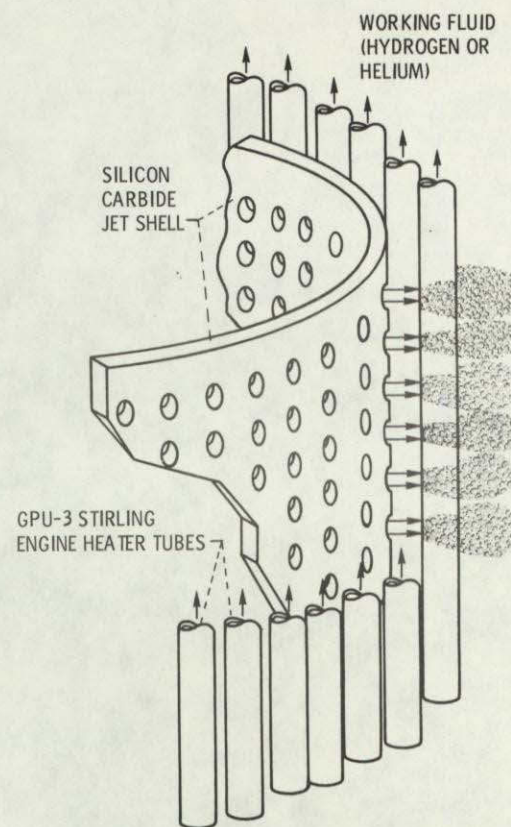
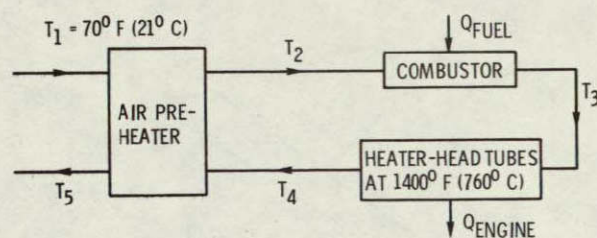


Figure 16. - Schematic of jet impingement concept.



	REFERENCE CASE	JET IMPINGEMENT
CONVECTION COEFFICIENT, Btu/hr ft ² °F (W/m ² °C)	60 (340)	120 (680)
T ₂ , °F (°C)	1783 (973)	1314 (712)
T ₃ , °F (°C)	3439 (1893)	3053 (1678)
T ₄ , °F (°C)	2239 (1226)	1645 (896)
T ₅ , °F (°C)	526 (274)	401 (205)

Figure 17. - Calculated combustion-gas temperatures for GPU-3 Stirling engine. Reference-case conditions: air-fuel ratio, 35; air-plus-fuel mass flow rate, 197 lb/hr (24.9 g/sec); preheater effectiveness, 80 percent; engine output, 8.4 hp (6.3 kW); fuel input, 39.9 hp (29.9 kW); input to engine, 26.9 hp (22.2 kW).

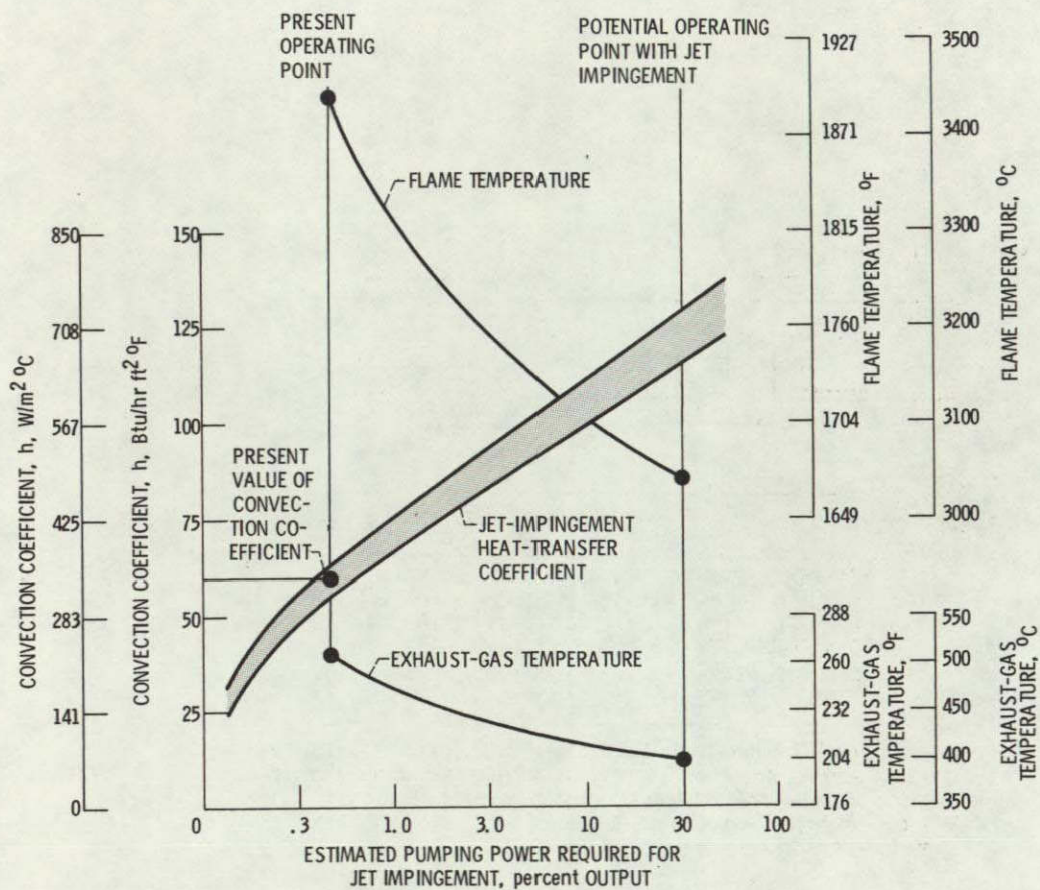
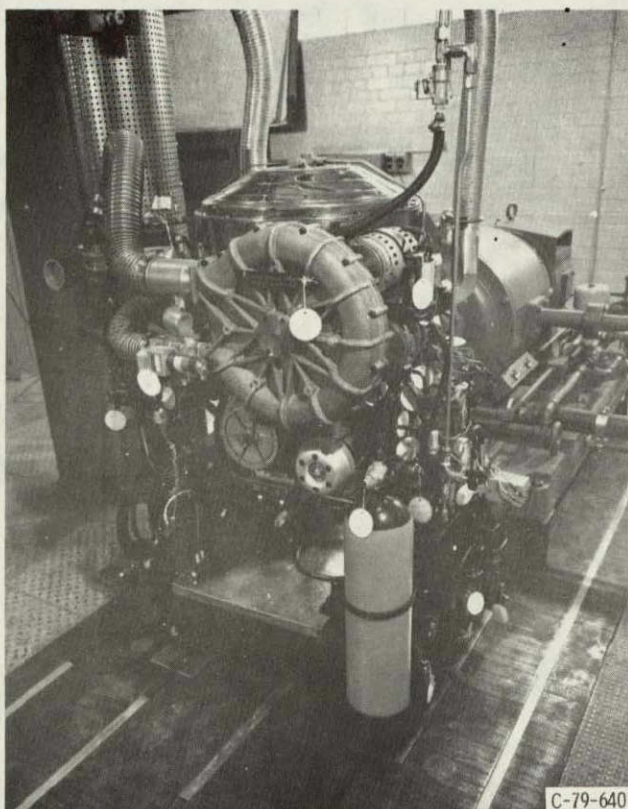
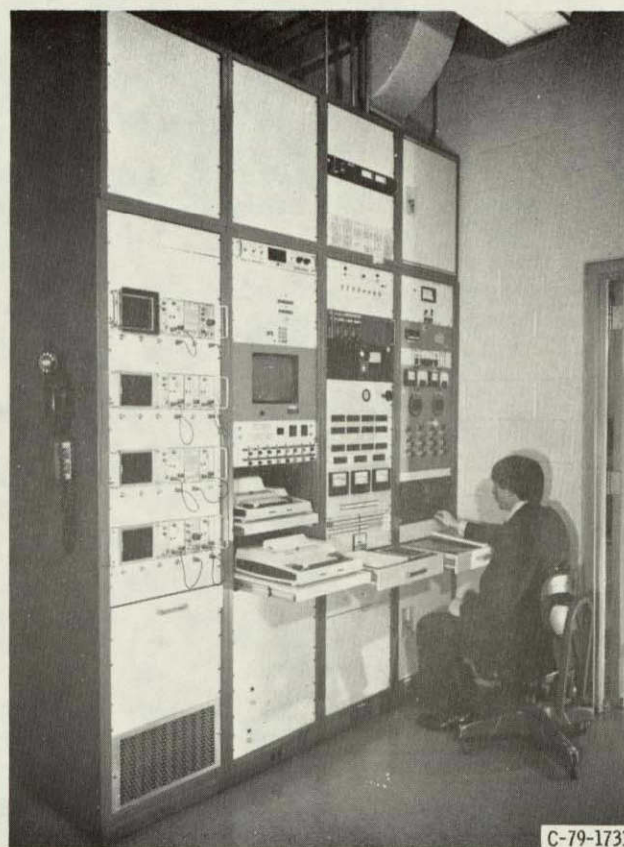


Figure 18. - Potential performance improvement of GPU-3 Stirling engine using jet impingement. Engine output, 8.4 hp (6.3 kW).



C-79-640

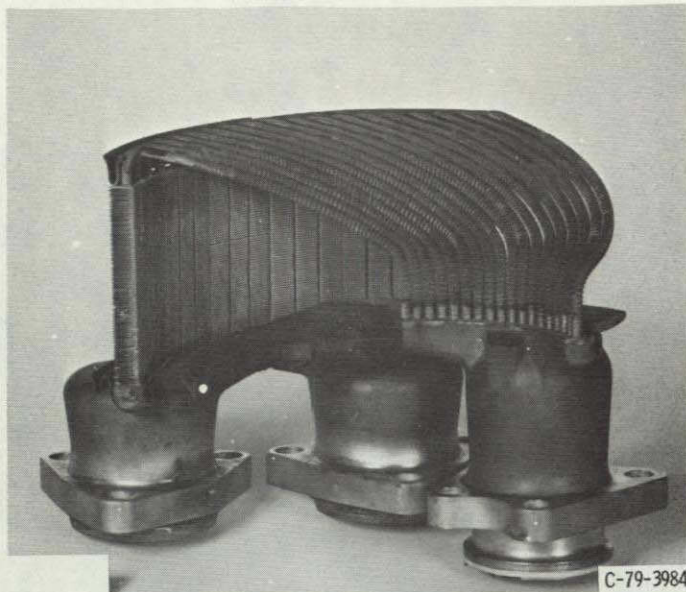
Figure 19. - United Stirling P-40 Stirling engine and dynamometer.



C-79-1733

Figure 20. - Control room for P-40 Stirling engine.

ORIGINAL PAGE IS
OF POOR QUALITY



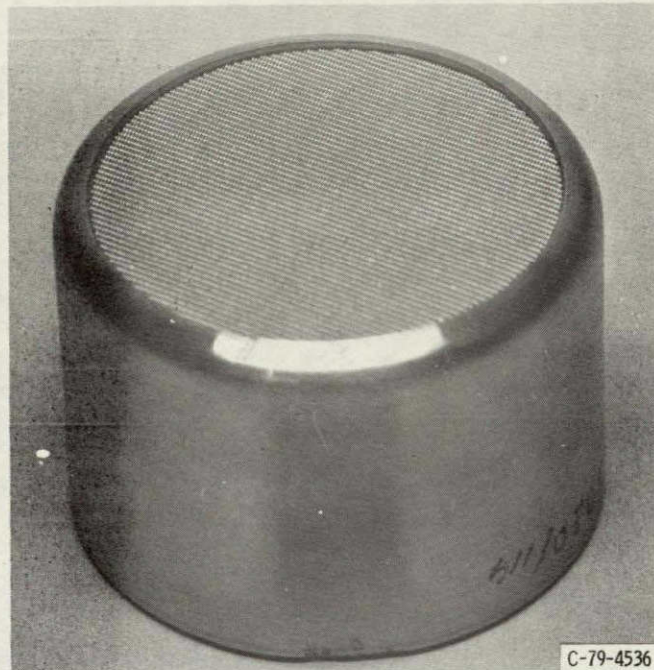
C-79-3984

Figure 21. - Heater-head quadrant from P-40 Stirling engine.



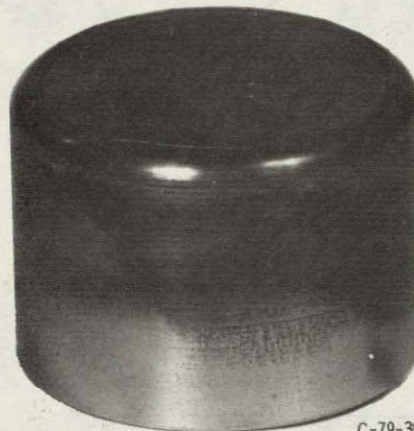
C-79-3983

Figure 22. - Underside of heater-head quadrant for P-40 Stirling engine, showing engine components.



C-79-4536

Figure 23. - P-40 stacked-screen regenerator before operation in engine.



C-79-3990

Figure 24. - P-40 stacked-screen regenerator after operation in engine.

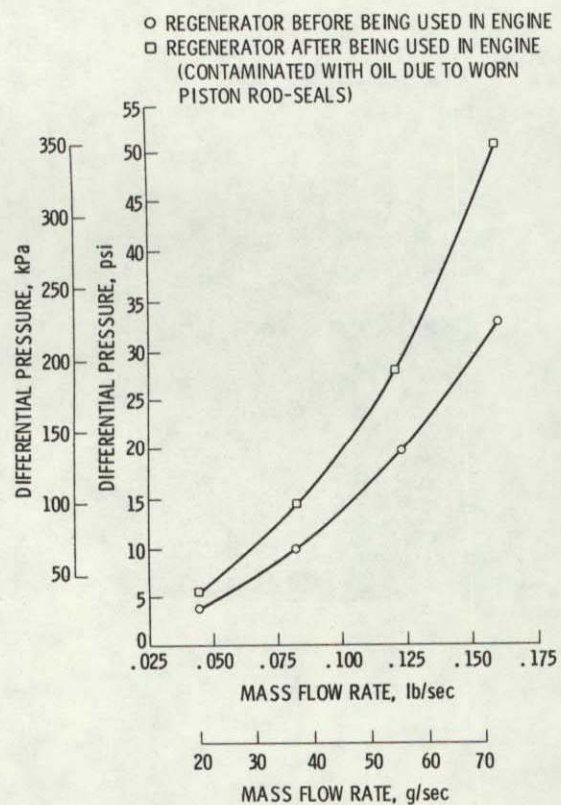


Figure 25. - Pressure drop characteristics of P-40 engine regenerators. Working fluid, air; upstream pressure, 110 psi (758 kPa); upstream temperature, 75° F (24° C).

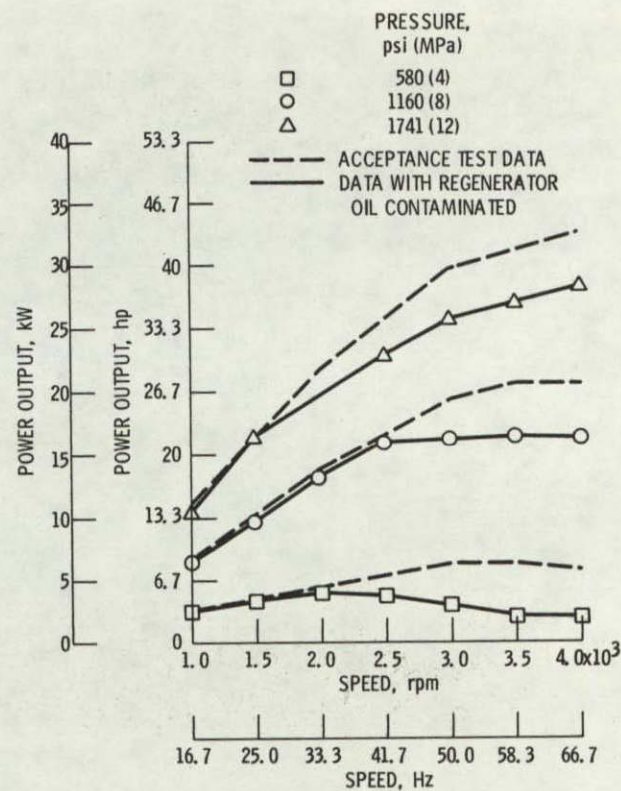


Figure 26. - P-40 brake power output as function of engine speed. Working fluid, hydrogen; heater-tube temperature, 1328° F (720° C); cooling-water inlet temperature, 122° F (50° C).

1 Report No NASA TM-81442		2 Government Accession No		3 Recipient's Catalog No	
4 Title and Subtitle OVERVIEW OF A STIRLING ENGINE TEST PROJECT				5 Report Date	
				6 Performing Organization Code	
7 Author(s) Jack G. Slaby				8 Performing Organization Report No E-362	
				10 Work Unit No	
9 Performing Organization Name and Address National Aeronautics and Space Administration Lewis Research Center Cleveland, Ohio 44135				11 Contract or Grant No	
				13 Type of Report and Period Covered Technical Memorandum	
12 Sponsoring Agency Name and Address U.S. Department of Energy Transportation Energy Conservation Division Washington, D.C. 20545				14 Sponsoring Agency Code DOE/NASA/1040-80/12	
15 Supplementary Notes Prepared under Interagency Agreement EC-77-A-31-1040. Prepared for Fifth International Automotive Propulsion Systems Symposium, Dearborn, Michigan, April 14-18, 1980.					
16 Abstract The NASA Lewis Research Center has overall project management responsibility for the Department of Energy Stirling Engine Highway Vehicle Systems Program. As part of this program the Lewis Research Center is conducting tests on three Stirling engines ranging in size from 1.33 to 53 horsepower (1 to 40 kW). The results of these tests are contributing to the development of a broad base of Stirling engine technology. In addition, the tests are directed toward developing alternative, backup component concepts to improve engine efficiency and performance or to reduce costs. Some of the activities include investigating attractive concepts and materials for cooler-regenerator units, installing a jet impingement device on a Stirling engine to determine its potential for improved engine performance, and presenting performance maps for initial characterization of Stirling engines. This report presents some of the experimental results to date and predictions of results of tests that will be conducted on these Stirling engines.					
17 Key Words (Suggested by Author(s)) Stirling engine; Regenerators, Heat engine; Engine testing; Jet impingement; Heat transfer				18 Distribution Statement Unclassified - unlimited STAR Category 44 DOE Category UC-96	
19 Security Classif (of this report) Unclassified		20 Security Classif (of this page) Unclassified		22 Price*	

* For sale by the National Technical Information Service, Springfield, Virginia 22161